An Interleaved PFM *LLC* Resonant Converter With Phase-Shift Compensation

Koji Murata, *Student Member, IEEE*, and Fujio Kurokawa, *Fellow, IEEE*

***Abstract*—The interleaved structure of *LLC* resonant converter with the phase-shift modulation (PSM) is presented and then its optimum operating region is discussed. The *LLC* resonant converters can achieve zero-voltage switching (ZVS) of the primary switches and zero-current switching (ZCS) of the secondary switches. However, the secondary peak current is large due to the discontinuous conduction mode (DCM). The interleaved PFM *LLC* resonant converter has difficulty in synchronizing switching instants among phases owing to the parameter mismatch of resonant circuits. In the proposed method, the current unbalance caused by the parameter mismatch is compensated by PSM. It is confirmed that the proposed method achieves lower peak current even when there is parameter mismatch and that the operation of below resonant frequency is suitable, both of which are simulated and experimentally verified.**

***Index Terms*—Interleave, *LLC* resonant converter, pulse frequency modulation (PFM), phase-shift modulation (PSM).**

I. Introduction

LLC resonant converters have been studied for front-end converters [1], [2]. It can operate at the resonant frequency under the nominal operating condition, which is the optimum operating point for resonant converters while it can meet the hold-up time requirement without any auxiliary circuit. In recent years, *LLC* resonant converters in the renewable energy system have been studied [3], [4]. The requirements for those *LLC* resonant converters are different from the requirements for front-end converters. For the front-end converter, discontinuous conduction mode (DCM) region or boost gain region of *LLC* resonant converter is used to satisfy the hold-up requirement.

In the renewable energy system, the input voltage of power converter varies depending on the amount of wind, the solar radiation and the temperature. The *LLC* resonant converter must operate in a wide frequency range to satisfy the wide input voltage range requirement [3]. Therefore, not only the operation at the series resonant frequency but also the operation below the series resonant frequency must be considered.

The *LLC* resonant converter has advantages over the conventional series resonant converter. Although the conventional series resonant converter has a problem of light load regulation, the *LLC* resonant converter achieves the light load regulation and the zero-voltage switching (ZVS) at an entire load range by utilizing the magnetizing inductance of a transformer [1]. The secondary switches of *LLC* resonant converter can operate at zero-current switching (ZCS) due to the DCM or boundary conduction mode (BCM), which causes larger peak current. On the other hand, since the series resonant converter always operates above the series resonant frequency, the peak of secondary current is not large due to the continuous conduction mode (CCM). The large peak current shortens the lifetime of capacitors, which degrades the reliability of power converters. Therefore, it is critical to reduce the peak of secondary current in the *LLC* resonant converters.

A new topology having inductance filter is proposed to reduce secondary current ripples by smoothing the secondary current [5]. Although it can achieve lower ripples with the simple modification, it loses ZCS capability of secondary rectifiers. Another popular approach to reduce the secondary current ripples is the interleaving method of switching converters. Although the interleaving method for pulsewidth modulation (PWM) converters has been studied so far, it cannot be directly applied to the pulse frequency modulation (PFM) converters. The switching frequencies of each converter in parallel must be synchronized for the interleaved operation. The parameter mismatch of each phase in *LLC* resonant circuit causes different gain characteristics at a synchronized switching frequency, which leads to the current unbalance among phases.

Many studies have been done on the interleaving method of *LLC* resonant converter [6]–[16]. The impacts of parameter mismatch of resonant circuit are discussed in [6]–[10]. The design method to improve the current balance is presented in [6]. In [7], a frequency-controlled current balancing method is proposed. Since the operating point is determined by the designed parameters, it cannot tightly regulate the output voltage and cannot achieve a wide input voltage range. Adaptive voltage position (AVP) for current balancing of the interleaved *LLC* resonant converter is proposed in [8]. The operating point also depends on the circuit parameters. Therefore, the wide input voltage cannot be achieved. In [9] and [10], since the parameter mismatch among phases of resonant circuit is compensated by varying the output voltages of power factor correction (PFC) circuit as the front stage, the PFCs must be placed in front of each phase of the interleaved *LLC* resonant converters. The series-input and parallel-output connection is proposed and analyzed in [11] and [12]. Although it can achieve secondary current balances, the input current is the same as that in the single-phase *LLC* resonant converter. Thus, the load capacity cannot be increased. In [13], multiphase *LLC* resonant converter with star connection is proposed. It balances the mean value of primary current. This configuration cannot operate with the redundancy operation.

Manuscript received January 28, 2015; revised March 13, 2015; accepted April 14, 2015. Date of publication April 29, 2015; date of current version November 16, 2015. Recommended for publication by Associate Editor V. Agarwal.

The authors are with Nagasaki University, Nagasaki 852-8521, Japan (e-mail: ijok64@gmail.com; fkurokaw@nagasaki-u.ac.jp).

Digital Object Identifier 10.1109/TPEL.2015.2427735

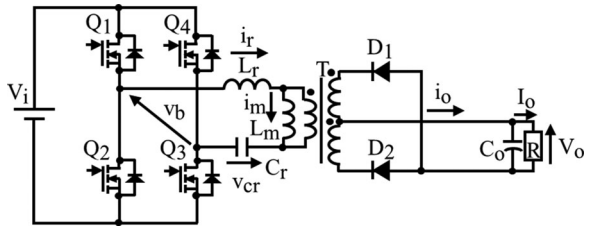

Fig. 1. Configuration of full-bridge LLC resonant converter.

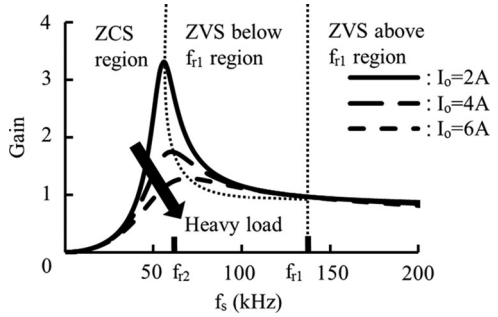

Fig. 2. Gain characteristics of *LLC* resonant circuit.

An interleaving method with a current-controlled inductor is proposed in [14]. The interleaving method tuning the resonant frequency is proposed for constant frequency operation in [15]. The output voltage and current balance is controlled by full-wave switch-controlled capacitors (SCCs). In [16], the half-wave SCCs for multiphase PFM *LLC* resonant converters is proposed. Taking the aforementioned factor into consideration, the interleaved structure that can operate at synchronous switching frequencies without any auxiliary circuit and that is also capable of redundancy operation is required.

In this paper, an interleaved structure of PFM *LLC* resonant converters without any auxiliary circuit is proposed and its optimum operating region is discussed. In the proposed method, the influence of parameter mismatch is compensated by the duty ratio control using the phase-shift modulation (PSM). Thus, the switching instants among phases can be synchronized without any auxiliary circuit. Furthermore, it can also operate at redundancy operation. Section II explains the operation principle of an interleaved structure of PFM *LLC* resonant converter with PSM. The effect of PSM on efficiency and peak current is studied in Section II. The interleaved structure is explained in section IV. The simulation and experimental results of single-phase and interleaved structure without PSM and interleaved structure with PSM are given in Section VI. The conclusion will be presented in Section V.

II. Operation Principle

Fig. 1 shows the circuit configuration of full-bridge *LLC* resonant converter. The full-bridge circuit consists of switches Q_1 through Q_4. The *LLC* resonant circuit consists of the resonant inductance L_r, magnetizing inductance L_m, and the resonant capacitor C_r. D_1 and D_2 are the rectifiers. C_o is the output capacitor. i_r indicates the current flowing through L_r. i_m indicates the magnetizing current of transformer. v_b indicates the output voltage of full-bridge circuit. i_o indicates the secondary current of transformer. I_o indicates the load current.

Fig. 2 shows the gain characteristics of *LLC* resonant circuit as a function of the switching frequency. The resonant frequencies f_{r1} and f_{r2} are expressed as (1) and (2), respectively. The operating region of *LLC* resonant converter is classified into three regions: ZCS region, ZVS below f_{r1} region, and ZVS above f_{r1} region. The operation in ZCS region is avoided because of the hard switching turn-on. Thus, the ZVS region for primary switches is chosen as a desired operating region for *LLC* resonant converter. The boundary of ZVS and ZCS is located between the frequency f_{r1} and f_{r2}, depending on the load conditions. The boundary approaches to f_{r1} with the increase of load current.

In the ZVS below f_{r1} region, the primary switches operate with ZVS, while the secondary switch operates with soft commutation. Due to the discontinuous conduction of secondary current, the peak current in the secondary side is larger than that in the ZVS above f_{r1} region. The variation of switching frequency has a great effect on the gain characteristics of resonant circuit. Thus, the gain of resonant circuit can vary with a narrow switching frequency variation. In the above f_{r1} region, the primary switches turn off before the secondary current decreases to zero. Although the peak current is smaller than that in ZVS below f_{r1} region, the secondary current differs from the sinusoidal shape. Furthermore, since the variation of switching frequency has less effect on gain characteristics of resonant circuit, the operation above frequency f_{r1} is not optimum for wide input or output range converters.

$$f_{r1} = \frac{1}{2\pi\sqrt{C_r \cdot L_r}} \tag{1}$$

$$f_{r2} = \frac{1}{2\pi\sqrt{C_r\,(L_r + L_m)}}. \tag{2}$$

Fig. 3(a) describes the waveforms of the PFM *LLC* resonant converter operating below f_{r1}. $T_{\rm on}$ indicates the on-time of signals for switches Q_1 through Q_4. D_p indicates the duty ratio of full-bridge circuit. T_c indicates the conduction time of secondary current.

$[t_0 - t_1]$: The resonant inductance L_r and the resonant capacitor C_r resonates. The magnetizing inductance L_m is clamped by the output voltage. When the primary resonant current i_r decreases to the current i_m, the secondary current $i_{\rm o}$ decreases to zero.

$[t_1 - t_2]$: The output voltage of full-bridge circuit v_b, which is the input voltage of resonant circuit, equals input voltage V_i. The capacitor C_r resonates with resonant inductance L_r and magnetizing inductance L_m. The energy is stored in resonant circuit. This interval ends when switch Q_3 turns off.

$[t_2 - t_3]$: Switches Q_1 through Q_4 are off. The parasitic capacitance of switch of Q_1, Q_3 and Q_2, Q_4 are charged and discharged to achieve ZVS, respectively.

Fig. 3(b) describes the waveforms of PSM *LLC* resonant converter when the $D_pT_{\rm on}$ is longer than the conduction time of secondary current T_c. This mode exists when the input voltage

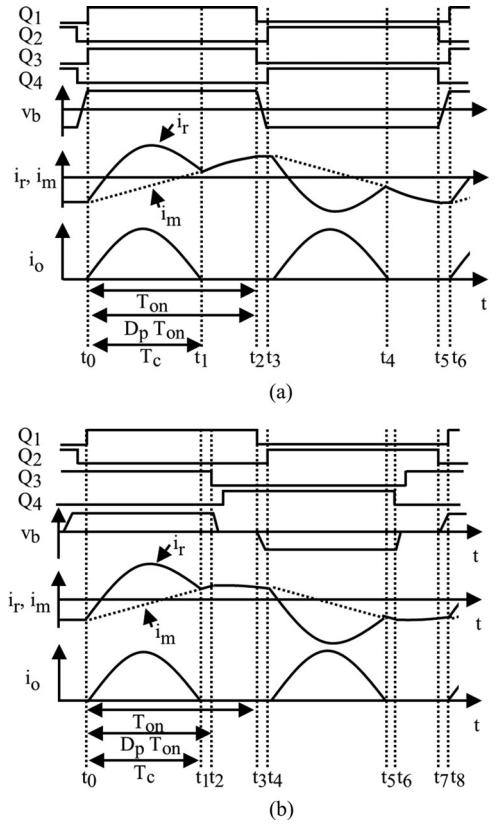

Fig. 3. Operating principle of *LLC* resonant converter operating below f_{r1}. (a) Without PSM. (b) With PSM.

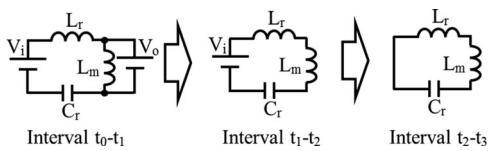

Fig. 4. Equivalent circuit of PSM *LLC* resonant converter operating below f_{r1}.

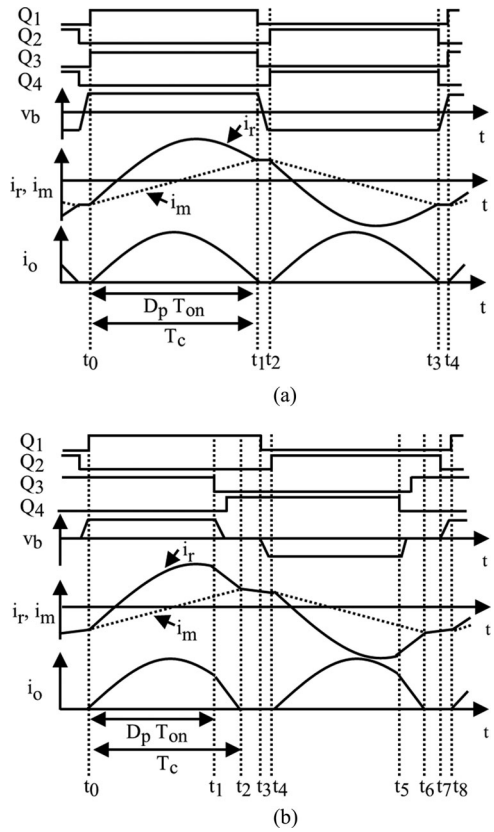

Fig. 5. Operating principle of *LLC* resonant converter operating at f_{r1}. (a) Without PSM. (b) With PSM.

is low, or lower switching frequency region of below f_{r1}.The operating principle is as follows.

$[t_0 - t_1]$: The operation during this interval is the same as PFM *LLC* resonant converters. The secondary current decreases to zero with soft commutation.

$[t_1 - t_2]$: Although the operating principle is the same as PFM *LLC* resonant converter, the width of this interval is determined by the duty ratio D_p of PSM. This interval ends when switch Q_3 turns off.

$[t_2 - t_3]$: The parasitic capacitance of switches Q_3 and Q_4 are charged and discharged, respectively. Then the switch Q_4 is turned-on with ZVS. Switches Q_1 and Q_4 are on. The input source is disconnected from the resonant circuit in this interval so that the voltage v_b is zero. The PSM decreases the energy stored in resonant circuit compared to the PFM *LLC* resonant converter. At t_3, the switch Q_1 turns off.

$[t_3 - t_4]$: Both switches Q_1 and Q_2 are off. The parasitic capacitance of switches Q_1 and Q_2 are charged and discharged, respectively. At t_4, switch Q_2 turns on with ZVS. Then the next half switching cycle starts. The operating principle of the interval $t_4 - t_8$ is the same as that of the interval $t0 - t4$. The transition of equivalent circuits is shown in Fig. 4. The dead time interval is omitted for the simplicity.

Fig. 5(a) describes the waveforms of PFM *LLC* resonant converter operating at the resonant frequency f_{r1}.

$[t_0 - t_1]$: The resonant inductance L_r and the resonant capacitor C_r resonate. The magnetizing inductance L_m is clamped by the output voltage. This interval ends when the current i_r decreases to the current i_m.

$[t_1 - t_2]$: Switches Q_1 through Q_4 are off. The stored energy in the parasitic capacitance of switch Q_1, Q_3 and Q_2, Q_4 are charged and discharged, respectively.

The waveforms of PSM *LLC* resonant converter in the case of $T_c > D_p T_{\rm on}$ are described in Fig. 5(b). When the on time of full-bridge circuit $D_p T_{\rm on}$ is shorter than the conduction time of secondary current T_c, the voltage v_b becomes zero before the current i_o decreases to zero. The secondary current reflected to the primary side is rapidly decreased by PSM. That is, the period that energy is transferred to the secondary side is reduced. The operating principle is as follows.

$[t_0 - t_1]$: The operating principle during this interval is the same as PFM *LLC* resonant converter. In the PSM, the driving signals for Q_3 and Q_4 are shifted from the driving signal for Q_1 and Q_2, respectively. When the switch Q_3 turns off, this interval ends.

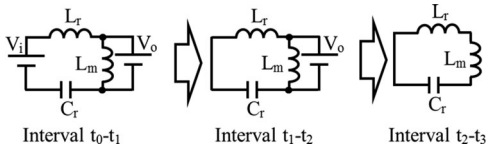

Fig. 6. Equivalent circuit of PSM *LLC* resonant converter operating at f_{r1}.

$[t_1 - t_2]$: The stored energy in the parasitic capacitance of switch Q_3 and Q_4 are charged and discharged, respectively. Then the switch Q_4 turns on with ZVS. During this interval, although the voltage v_b becomes zero, the resonant current i_r is still larger than the magnetizing current i_m. Thus, the energy is transferred from the primary to the secondary side. The slope of current i_r is expressed as $[nV_o + v_{cr}(t_1)]/L_r$. The current i_m continues to increase because the magnetizing inductance L_m is still clamped to the output voltage. This interval ends when the resonant current i_r decreases to the current i_m.

$[t_2 - t_3]$: Rectifiers D_1 and D_2 are off. No energy is transferred from the primary to the secondary side in this period. The magnetizing inductance L_m resonates with L_r and C_r.

$[t_3 - t_4]$: At t_3, switch Q_1 turns off. The parasitic capacitance of switches Q_1 and Q_2 are charged and discharged to achieve ZVS, respectively. The transition of equivalent circuit is shown in Fig. 6. The dead time interval is omitted for simplicity.

At the heavy load condition, the current decreases during $v_b = 0$ in both below and above f_{r1} regions. However, each of phases of interleaved *LLC* resonant converter operates at lighter loads because the current is distributed among phases. Under the light load condition, even when PSM is applied, the current i_r is kept almost constant during $v_b = 0$, which is enough to charge and discharge the parasitic capacitance of switches to achieve ZVS. For this reason, the impact of PSM on the ZVS condition is small in this application.

III. Effect of PSM

Figs. 7 and 8 show the effect of duty ratio in the case of $V_i = 30$ and 50 V, respectively. As explained in the previous section, the operating principle of proposed full-bridge *LLC* resonant converter for interleaving is classified into two modes. When the conduction time of secondary current T_c is shorter than the on-time of full-bridge circuit $D_p T_{\rm on}$, which happens at lower input voltage, the shape of secondary current is kept sinusoidal. The shape of secondary current is changed when the time T_c is longer than the time $D_p T_{\rm on}$, which happens at higher input voltage. Fig. 7(a) plots the efficiency of phase-shifted full-bridge *LLC* resonant converter when the input voltage and output voltage are 30 and 5 V, respectively. The corresponding variations of switching frequency are shown in Fig. 7(b). The increase of efficiency is observed at light load due to the reduction of peak of magnetizing current. Fig. 7(c) shows the peak of secondary current i_o as a function of duty ratio D_p. As it can be seen, the peak current remains constant value even when duty ratio decreases because the soft commutation of secondary current in a sinusoidal manner is maintained. Thus, in this operating region, there is no negative effect by PSM. The soft-commutation of

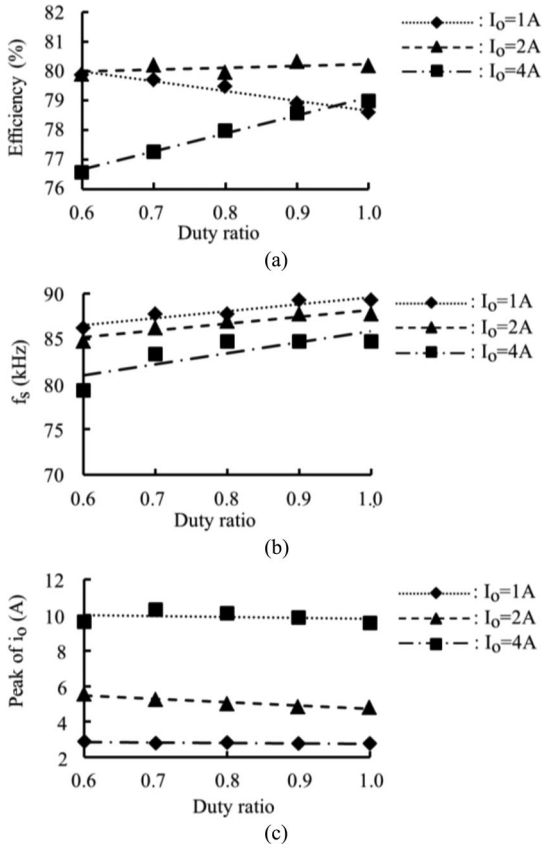

Fig. 7. Effect of duty ratio in the case of $V_i = 30$ V. (a) Efficiency as a function of duty ratio. (b) Switching frequency variation. (c) Peak of i_o as a function of duty ratio.

secondary current in a sinusoidal manner is maintained in case of $D_p T_{on} > T_c$. The ZCS turn-off of secondary switches of the *LLC* resonant converter is achieved at any $D_p T_{\rm on}$ owing to the discontinuous conduction of the secondary side current.

The efficiency of phase-shift-modulated full-bridge *LLC* resonant converter as a function of duty ratio in the case of $Vi = 50$ V is plotted in Fig. 8(a). The corresponding variations of switching frequencies are shown in Fig. 8(b). The input voltage and the output voltage are 50 and 5 V, respectively. At the light-load condition, the improvement of efficiency is observed due to the reduction of peak of magnetizing current. At the heavy load, the efficiency is decreased. The peak of primary and secondary current is increased by PSM. The simulated peak value of secondary current i_o as a function of duty ratio is shown in Fig. 8(c). In this operating region, PSM directly affects the current transferred to the secondary side. Thus, in this operating region, the secondary current differs from the sinusoidal shapes and its peak current increases as duty ratio decreases. The operation of below f_{r1} region is recommended from the view point of reduction of peak current and soft-commutation.

IV. Interleaved Operation

Fig. 9 shows the circuit configuration of interleaved full-bridge *LLC* resonant converter. Both input and output are connected in parallel, respectively. The diodes D_1 through D_4 block

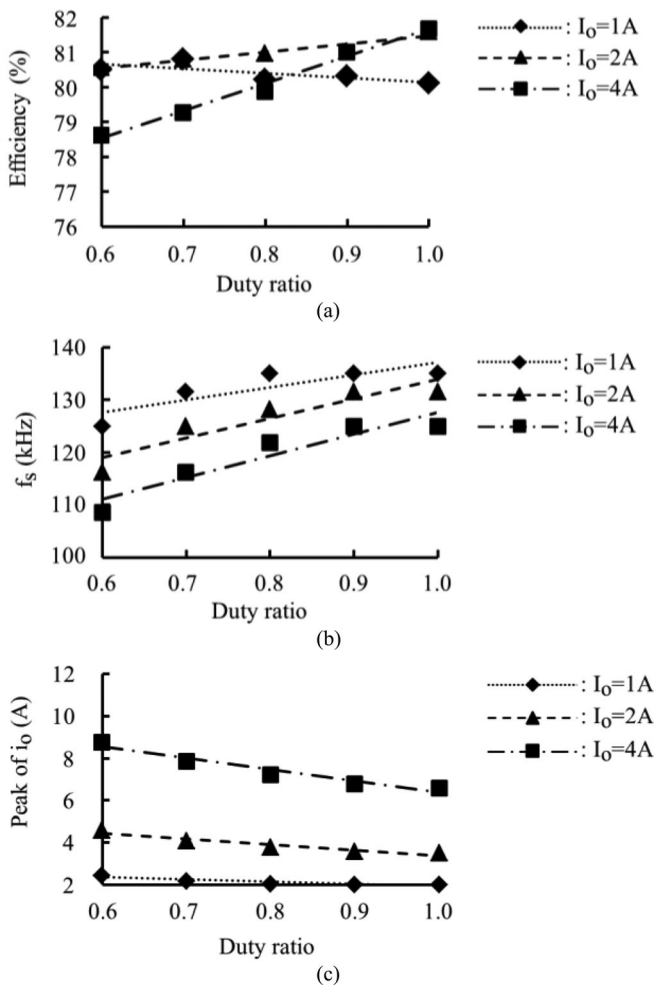

Fig. 8. Effect of duty ratio in the case of $V_i = 50$ V. (a) Efficiency as a function of duty ratio. (b) Switching frequency variation. (c) Peak of i_o as a function of duty ratio.

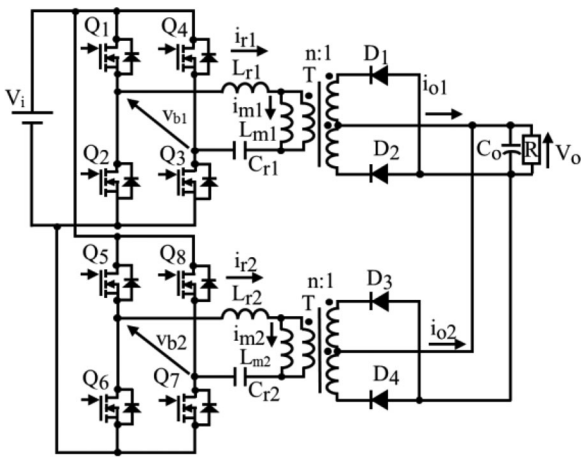

Fig. 9. Interleaved *LLC* resonant converter.

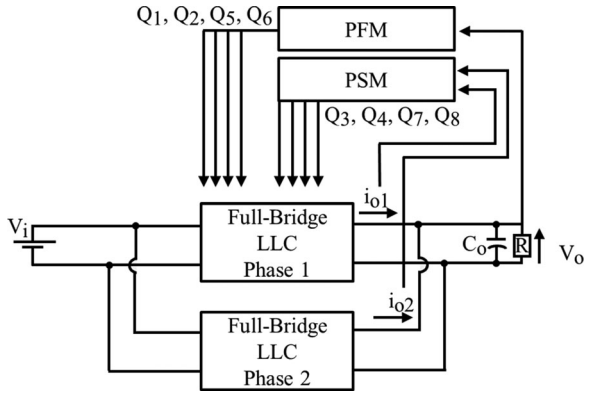

Fig. 10. Proposed interleaved *LLC* resonant converter.

the reverse current so that there is no path circulating current flows through. Therefore, it is also capable of the redundancy operation. When the *LLC* resonant circuits of both phases are identical, currents in both phases are well balanced with a synchronized switching frequency. When there is parameter mismatch among phases, current unbalance can occur at a synchronized switching frequency. With PSM, driving signals for Q_1 and Q_2 are phase shifted from Q_3 and Q_4. Thus, PSM is applied so that current unbalance caused by parameter mismatch can be improved at a synchronized switching frequency.

Fig. 10 shows the configuration of the proposed interleaving method for the full-bridge *LLC* resonant converter. The output voltage is regulated by the PFM, while the duty ratio control using PSM is performed for compensating the gain mismatch of two phases of *LLC* resonant circuit. The current sensor for the secondary current is required to change the duty ratio D_p.

Fig. 11 shows the operating principle of interleaved PFM *LLC* resonant converter with the PSM compensation when the phase 1 has larger gain of resonant circuit. v_{b1} and v_{b2} are the output voltage of full-bridge circuit in phases 1 and 2, respectively. T_a indicates the shifted width of interleaved operation. i_{r1} and i_{r2} are primary current in phases 1 and 2, respectively. i_{o1} and i_{o2} are secondary current of transformer in phases 1 and 2. At t_0, switch Q_1 turns on. The power is transferred from the primary side to the secondary side of phase 1. At t_1, switch Q_5 in phase 2 turns on. The power is transferred from the primary side to the secondary side of phase 2.

The power each phase transfers is half of single phase in both primary and secondary sides. PSM control is applied to the phase 1. At t_2, switch Q_3 turns off. The output voltage of full-bridge circuit v_{b1} becomes zero. Thus, the magnetizing current is decreased compared to that in PFM. The energy stored in resonant circuit is also decreased. Thus, the current balance is improved even when there are parameter mismatch between interleaved phases. At t_3, the next half cycle starts.

When the current unbalance occurs, the PSM is applied to the phase that has larger gain to decrease the gain. The required switching frequency changes according to that. In this case, the PFM decreases the switching frequency in order to increase the gain of the interleaved *LLC* resonant converter. Therefore,

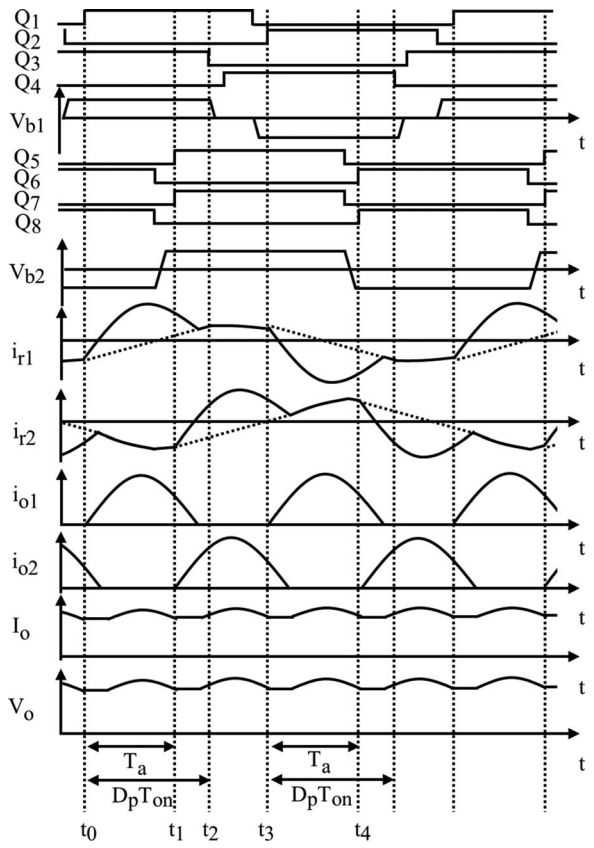

Fig. 11. Operating principle of interleaved *LLC* resonant converter with PSM operating below f_{r1}.

PFM must operate to compensate the deviation of output voltage caused by the PSM compensation.

V. Current Balance

The experimental prototype with parameter mismatch is built to confirm the validity of the proposed interleaved *LLC* resonant converter with PSM. The turn ratio of transformer n_1/n_2 is 9. The output voltage is 5 V. Both resonant capacitors C_{r1} and C_{r2} are 47 nF. The parameter errors between phases are made to investigate the validity of the proposed interleaved *LLC* resonant converter with PSM. The resonant inductances L_{r1} and L_{r2} are 36 and 34 μH, respectively. The magnetizing inductance L_{m1} and L_{m2} are 135 and 147 μH. The output capacitor C_o is 449 μF. The gain characteristics of resonant circuits of both phases derived from fundamental harmonic analysis (FHA) is shown in Fig. 12.

To verify the operation on both operating modes, current balances are investigated when the input voltages are 30 and 50 V, respectively. When the input voltage is 30 V, the conduction time T_c is shorter than the time $D_p T_{\rm on}$. In this case, the gain mismatch is compensated by reducing the magnetizing current i_m.

Fig. 13 shows the simulated waveforms of output voltage of full-bridge circuit v_{b1} and v_{b2}, primary resonant current i_{r1} and i_{r2}, and the secondary current i_{o1} and i_{o2} in the case of

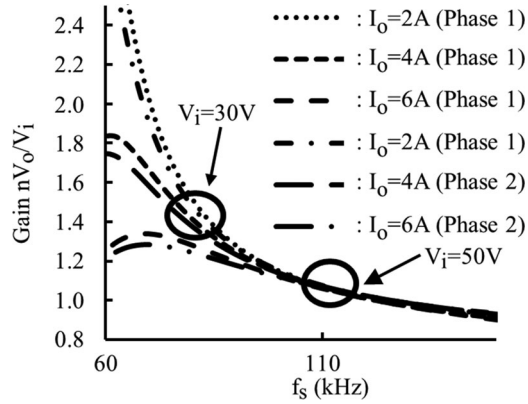

Fig. 12. DC gain characteristics of resonant circuit in phases 1 and 2.

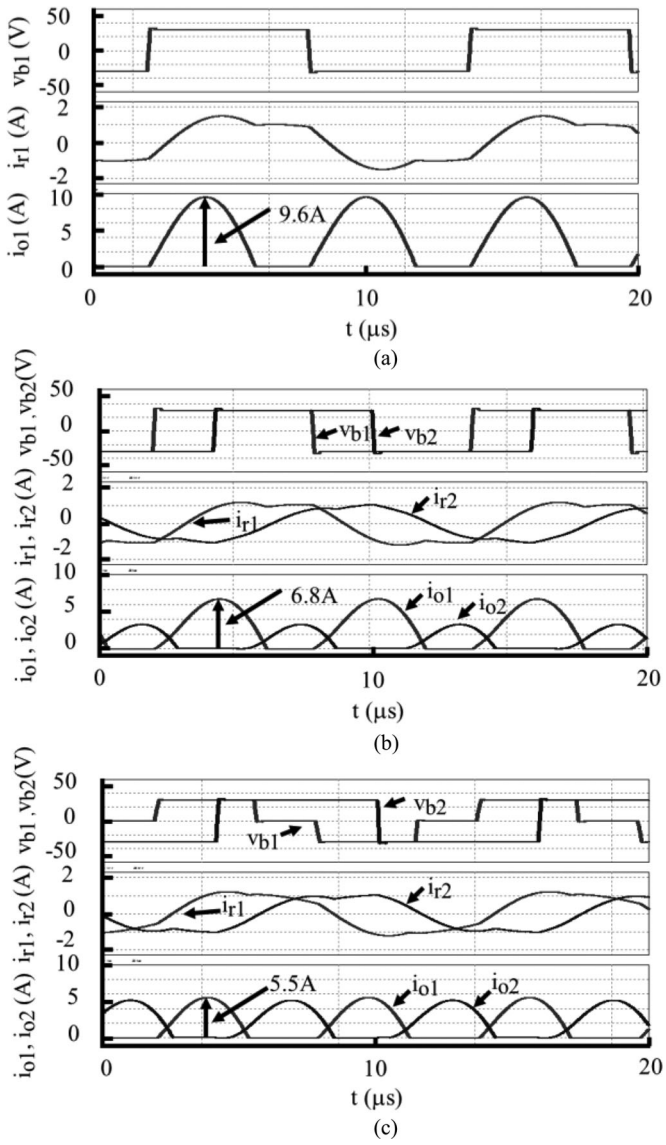

Fig. 13. Simulated waveform in the case of $V_i = 30$ V. (a) Single phase. (b) Without PSM. (c) With PSM.

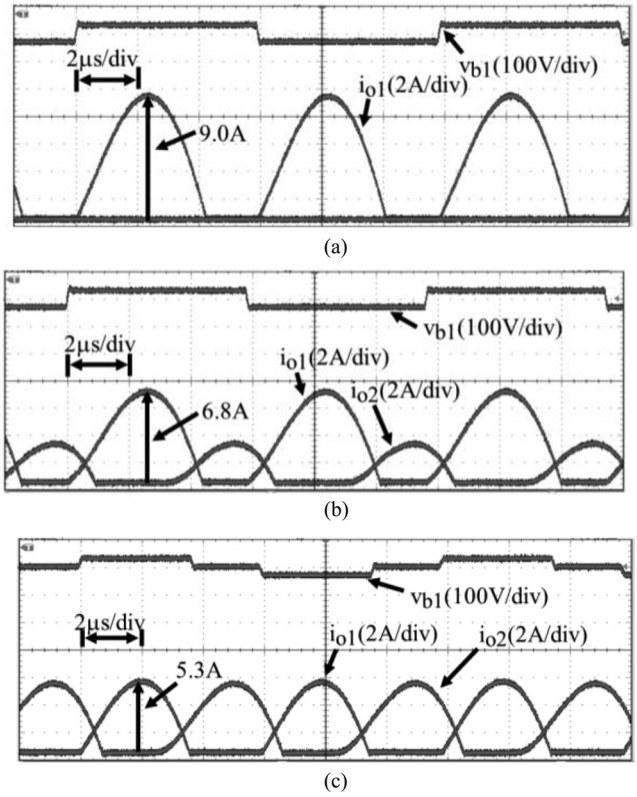

Fig. 14. Experimental waveforms in the case of $V_i = 30$ V. (a) Single phase. (b) Without PSM. (c) With PSM.

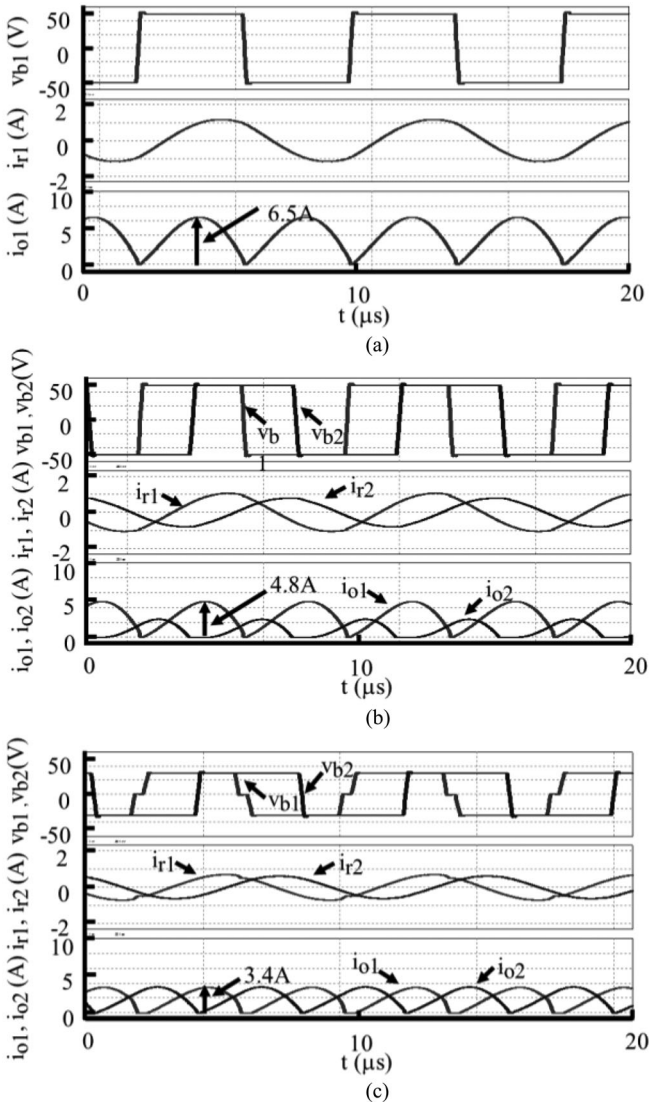

Fig. 15. Simulated waveform in the case of $V_i = 50$ V. (a) Single phase. (b) Without PSM. (c) With PSM.

$V_i = 30$ V. The PSIM is used as a simulator. The time step in the simulator is 1 ns. Fig. 13(a) shows the waveform of single-phase *LLC* resonant converter. The peak of output current is 9.6 A, which is more than twice of the output current of 4 A. Fig. 13(b) and (c) shows the simulated waveform with and without PSM, respectively. The peak of secondary current is reduced from 6.8 to 5.5 A with PSM. The corresponding experimental waveforms are shown in Fig. 14. In the proposed method with PSM, the duty ratio D_p is 0.6. As it can be seen, the peak current of single-phase and interleaved converter with and without PSM are 9.0, 6.8, and 5.3 A, respectively.

Fig. 15 shows the simulated waveform when the input voltage is 50 V. When the input voltage is 50 V, since the conduction time T_c is closer to the switching period, the secondary current balance is controlled by limiting the amount of the primary-reflected secondary current. The simulated waveforms of single-phase *LLC* resonant converter are shown in Fig. 15(a). The peak of secondary current i_o is 6.5 A. Fig. 15(b) and (c) shows the simulated waveforms of the interleaved *LLC* resonant converter with and without PSM, respectively. The peak of secondary current is reduced from 4.8 to 3.4 A. Fig. 16 shows the corresponding experimental waveforms. Fig. 16(a) shows the waveforms of single-phase *LLC* resonant converter. The peak of secondary current i_o is 6.2 A. As shown in Fig. 16(b) and (c), the peak of secondary current is reduced from 4.1 to 3.8 A by combining PFM and PSM. The duty ratio D_p is 0.9 in the proposed method with PSM.

Fig. 17 plots the efficiency of single-phase *LLC* resonant converters, interleaved PFM, and proposed interleaved PFM *LLC* resonant converter. The efficiency of the interleaved converter at an arbitrary load should be approximately the average of efficiency of each phase at half of its load condition because the output current is distributed among phases. In the case of $I_o = 4$ A, the efficiency of both phases is 79%, whereas the efficiency of interleaved phases achieves 80%. Since the current flowing through each phase is a half of the single-phase converter, the efficiency of interleaved converter in the case of $I_o = 4$ A is almost equal to the single-phase converter in the case of $I_o = 2$ A. The efficiency of interleaved PFM converter without PSM in the case of $I_o = 2$ A is almost the same as the average of single-phase PFM converters in the case of $I_o = 1$ A. As explained in Fig. 7(a) in Section III, the efficiency of $I_o = 1$ A is increased by PSM. As shown in Fig. 7(b), the operating region with PSM is higher than the switching frequency without PSM. Therefore,

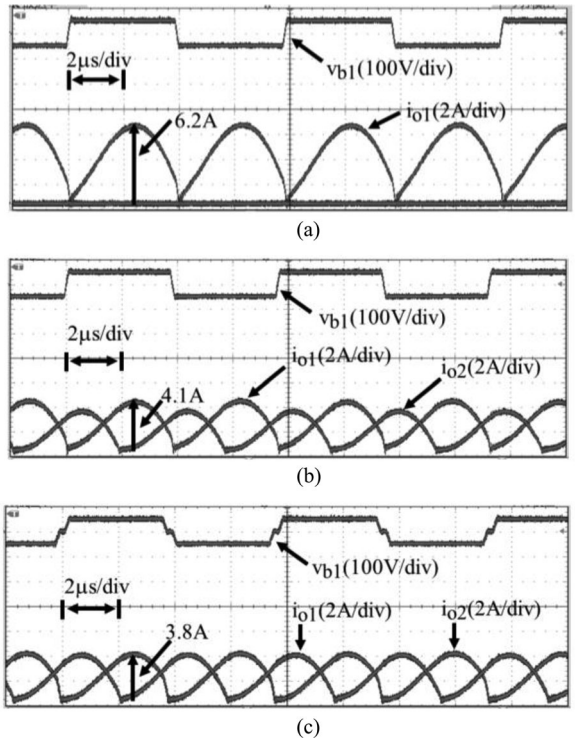

Fig. 16. Experimental waveforms in the case of $V_i = 50$ V. (a) Single phase. (b) Without PSM. (c) With PSM.

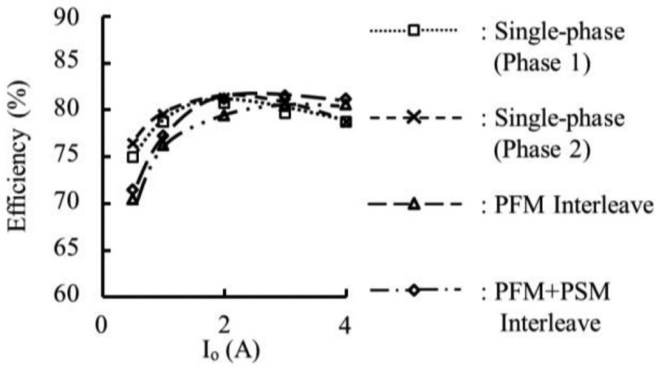

Fig. 17. Efficiency of LLC resonant converter.

the peak of magnetizing current that circulates in the primary side and the peak of secondary current are reduced. The efficiency of PFM+PSM interleaved *LLC* converter in the case of $I_o = 1$ A is higher than the average of efficiency of single-phase *LLC* converters in the case of $I_o = 0.5$ A.

VI. Conclusion

This paper presents the interleaved structure of *LLC* resonant converter with the PSM and then its optimum operating region is discussed. The parameter mismatch of resonant circuit is made to confirm the validity of the proposed method. It is confirmed that the proposed method using PSM can reduce the peak of secondary current with synchronized switching frequencies without any auxiliary circuit. The redundancy operation is also possible in this interleaved structure because there is no path that current circulates among phases. As the duty ratio of PSM decreases, the peak of secondary current increases due to the discontinuous conduction at higher switching frequency region. Furthermore, the shape of secondary current differs from sinusoidal shapes due to the lack of soft commutation of secondary switches by PSM. On the other hand, the shape of secondary current is almost not affected by PSM at lower switching frequency region. It is simulated and experimentally verified that the proposed method achieves a lower peak current even when there is parameter mismatch. It is also confirmed that the proposed method is suitable for the wide input or output voltage applications that operate below resonant frequency f_{r1}.

References

[1] B. Yang, F. C. Lee, A. J. Zhang, and G. Huang, "*LLC* resonant converter for front end dc/dc conversion," in *Proc. IEEE Appl. Power Electron. Conf.*, 2002, pp. 1108–1112.

[2] B. Lu, W. Liu, Y. Liang, F. C. Lee, and J. D. van Wyk, "Optimal design methodology for *LLC* resonant converter," in *Proc. IEEE Appl. Power Electron. Conf.*, 2006, pp. 533–538.

[3] H.-D. Gui, Z. Zhang, X-F He, and Y.-F. Liu, "A high voltage-gain LLC micro-converter with high efficiency in wide input range for PV applications," in *Proc. IEEE Appl. Power Electron. Conf.*, 2014, pp.637–642.

[4] G. Oriti, A. L. Julian, and T. D. Bailey, "PV power conditioning system with LLC resonant converter in DCM," in *Proc. IEEE Energy Convers. Congr. Expo.*, 2014, pp. 4262–4268.

[5] B. C. Hyeon and B. H. Cho, "Analysis and design of the LmC resonant converter for low output current ripple," *IEEE Trans. Ind. Electron.*, vol. 59, no. 7, pp. 2772–2780, Jul. 2012.

[6] B.-C. Kim, K.-B. Park, and G.-W. Moon, "Analysis and design of two-phase interleaved LLC resonant converter considering load sharing," in *Proc. IEEE Energy Convers. Congr. Expo.*, 2009, pp. 1141–1144.

[7] H. Figge, T. Grote, N. Froehleke, J. Boecker, and P. Ide, "Paralleling of LLC resonant converters using frequency controlled current balancing," in *Proc. IEEE Power Electron. Specialists Conf.*, 2008, pp. 1080–1085.

[8] F. Duan, M. Xu, X. Yang, and Y. Yao, "Asymmetrical interleaving strategy and AVP concept for interleaved LLC resonant DC/DC," in *Proc. IEEE Appl. Power Electron. Conf.*, 2014, pp. 2003–2010.

[9] H. Figge, T. Grote, F. Schafmeister, N. Fröhleke, and J. Böcker, "Two-phase interleaving configuration of the LLC resonant converter - Analysis and experimental evaluation," in *Proc. Ann. Conf. IEEE. Ind. Electron. Soc.*, 2013, pp. 1392–1397.

[10] H.-S. Kim, J.-W. Baek, M.-H. Ryu, J.-H. Kim, and J.-H. Jung, "The high-efficiency isolated ac–dc converter using the three-phase interleaved LLC resonant converter employing the Y-connected rectifier," *IEEE Trans. Power Electron.*, vol. 29, no. 8, pp. 4017–4028, Aug. 2014.

[11] B.-C. Kim, K.-B. Park, C.-E. Kim, and G.-W. Moon, "Load sharing characteristic of two-phase interleaved LLC resonant converter with parallel and series input structure," in *Proc. IEEE Energy Convers. Congr. Expo.*, 2009, pp. 750–753.

[12] G. Yang, P. Dubus, and D. Sadarnac, "Analysis of the load sharing characteristics of the series-parallel connected interleaved LLC resonant converter," in *Proc. IEEE Optim. Electr. Electron. Equip.*, 2012, pp. 798–805.

[13] E. Orietti, P. Mattavelli, G. Spiazzi, C. Adragna, and G. Gattavari, "Current sharing in three-phase LLC interleaved resonant converter," in *Proc. IEEE Energy Convers. Congr. Expo.*, 2009, pp. 1145–1152.

[14] E. Orietti, P. Mattavelli, G. Spiazzi, C. Adragna, and G. Gattavari, "Two-phase interleaved LLC resonant converter with current-controlled inductor," in *Proc. IEEE Brazilian Power Electron. Conf.*, 2009, pp. 289–304.

[15] Z. Hu, Y. Qiu, L. Wang, and Y.-F. Liu, "An interleaved LLC resonant converter operating at constant switching frequency," *IEEE Trans. Power Electron.*, vol. 29, no. 6, pp. 2931–2943, Jun. 2014.

[16] Z. Hu, Y. Qiu, Y.-F. Liu, and P. C. Sen, "An interleaving and load sharing method for multiphase LLC converters," in *Proc. IEEE Appl. Power Electron. Conf.*, 2013, pp. 1421–1428.

Koji Murata (S'10) was born in Japan in 1987. He received the B.S. and M.S. degrees in electrical and electronics engineering in 2010 and 2012, respectively, from Nagasaki University, Nagasaki, Japan, where he is currently working toward the Ph.D. degree.

His current research interests include digital control of switching converter and soft-switching converter.

Fujio Kurokawa (F'11) was born in Yamaguchi, Japan, in 1952. He received the B.S. degree in electronic engineering from the Fukuoka Institute of Technology, Fukuoka, Japan, in 1976, and the Dr.Eng. degree from Osaka Prefecture University, Sakai, Japan, in 1988.

Since 1984, he has been with Nagasaki University, where he is currently a Professor and Vice-Dean of Graduate School of Engineering. His current research interests include digital power, switching power supply for telecommunications, solar power supply, power plant control, and ion engine control for satellite.

Dr. Kurokawa is a Fellow of the Illuminating Engineering Institute of Japan and a Senior Member of the Institute of Electronics, Information and Communication Engineers of Japan, and the Institute of Electrical Engineers of Japan.